Available online at www.sciencedirect.com
SCIENCE DIRECT®
International Journal of Thermal Sciences 42 (2003) 57–62
International Journal of Thermal Sciences
www.elsevier.com/locate/ijts

Measurements of laminar mixed convection flow adjacent to an inclined surface with uniform wall heat flux

H.I. Abu-Mulaweh

Mechanical Engineering Department, Purdue University at Fort Wayne, 2101 E. Coliseum Blvd., Fort Wayne, IN 46805, USA

Received 16 August 2001; accepted 5 February 2002

Abstract

Measurements of laminar mixed convection flow adjacent to an inclined heated flat plate with uniform wall heat flux are reported. Laser-doppler velocimeter and cold wire anemometer were used to measure simultaneously the velocity and temperature distributions, respectively. Measurements of the air velocity and temperature distributions are presented for a range of buoyancy parameters $0 \leqslant \xi \leqslant 2.91$. It was found that both the mixed convection local Nusselt number and local friction coefficient increase as the buoyancy force increases (under the buoyancy assisting condition). The velocity field was found to be more sensitive to the buoyancy force than the thermal field. Predictions from both local similarity and local nonsimilarity models agree well with the experimental results for the thermal field, but only the predictions from the local nonsimilarity model agree favorably with the measured values for the flow field.

Keywords: Inclined surface; Uniform heat flux; Laminar; Convection; Mixed

1. Introduction

Flow and heat transfer characteristics of mixed convection air flow adjacent to a uniform heat flux surface is of considerable interest to engineers who deal with the design of electronics cooling equipments and cooling systems in nuclear power plants. Mixed convection flow and heat transfer in laminar boundary layer flows adjacent to vertical, inclined and horizontal surfaces have been examined by many investigators in the past (see, for example, Lin and Chen [1], Risbeck et al. [2], Kafoussias et al. [3], Hassanein et al. [4] and the references cited therein). However, the related experimental studies are limited in number (see, for example, Ramachandran et al. [5,6], Moharreri et al. [7], Abu-Mulaweh et al. [8] and the references cited therein). The majority of the published mixed convection measurements have been for uniform wall temperature boundary condition. A review of the open literature indicates that measurements in the laminar boundary layer mixed convection regime with uniform wall heat flux boundary condition are scarce. A lack of detailed measurements of flow and thermal fields in laminar mixed convection adjacent to an inclined surfaces with uniform wall heat flux has motivated the present study. Such detailed measurements are needed to validate numerical models.

This study was carried out to measure detailed temperature and velocity distributions and to obtain local Nusselt numbers in laminar air flow adjacent to an inclined flat plate (at 45 degrees) maintained at a uniform heat flux for the buoyancy-assisting case. This investigation is an extension of an earlier work by Abu-Mulaweh et al. [8]. Measurements are compared with predictions to validate existing numerical models.

2. Experimental apparatus and procedure

The measurements were carried out in an existing low-turbulence, open-circuit air tunnel which could be rotated and fixed at any desired inclination angle. The tunnel was oriented at an inclination angle $\phi = 45$ degrees, with air flowing in the upward direction along the tunnel. Details of the air tunnel have been described by Ramachandran et al. [5,6] and a schematic is shown in Fig. 1. The free stream velocity in the tunnel could be varied between

E-mail address: mulaweh@ipfw.edu (H.I. Abu-Mulaweh).

1290-0729/02/$ – see front matter
PII: S1290-0729(02)00007-8

Nomenclature

C_f	friction coefficient, $= \tau_w/(\rho u_\infty^2/2)$	u	mean streamwise velocity ..... $m{\cdot}s^{-1}$
Gr_x^*	modified local Grashof number, $= g\beta q_w x^4/kv^2$	u_∞	free stream velocity ..... $m{\cdot}s^{-1}$
g	gravitational acceleration ..... $m{\cdot}s^{-2}$	x, y	streamwise and transverse coordinates ..... m
h	local heat transfer coefficient, $= q_w/(T_w - T_\infty)$ ..... $W{\cdot}m^{-2}{\cdot}{}^\circ C^{-1}$	*Greek symbols*	
k	thermal conductivity ..... $W{\cdot}m^{-1}{\cdot}{}^\circ C^{-1}$	η	similarity parameter, $= y[u_\infty/(vx)]^{1/2}$
q_w	local surface heat flux ..... W	β	coefficient of thermal expansion ..... K^{-1}
Pr	Prandtl number, $= C_p\mu/k$	μ	dynamic viscosity ..... $kg{\cdot}m^{-1}{\cdot}s^{-1}$
Nu_x	local Nusselt number, $= hx/k$	θ	temperature difference, $= (T - T_\infty)$ ..... °C
Re_x	local Reynolds number, $= u_\infty x/v$	θ_w	temperature difference, $= (T_w - T_\infty)$ ..... °C
T	fluid temperature ..... °C	v	kinematic viscosity ..... $m^2{\cdot}s^{-1}$
T_∞	ambient temperature ..... °C	τ	wall shear stress, $= \mu(\partial u/\partial y)_{y=0}$
T_w	local wall temperature ..... °C	ξ	buoyancy parameter, $= Gr_x^*/Re_x^{5/2}$

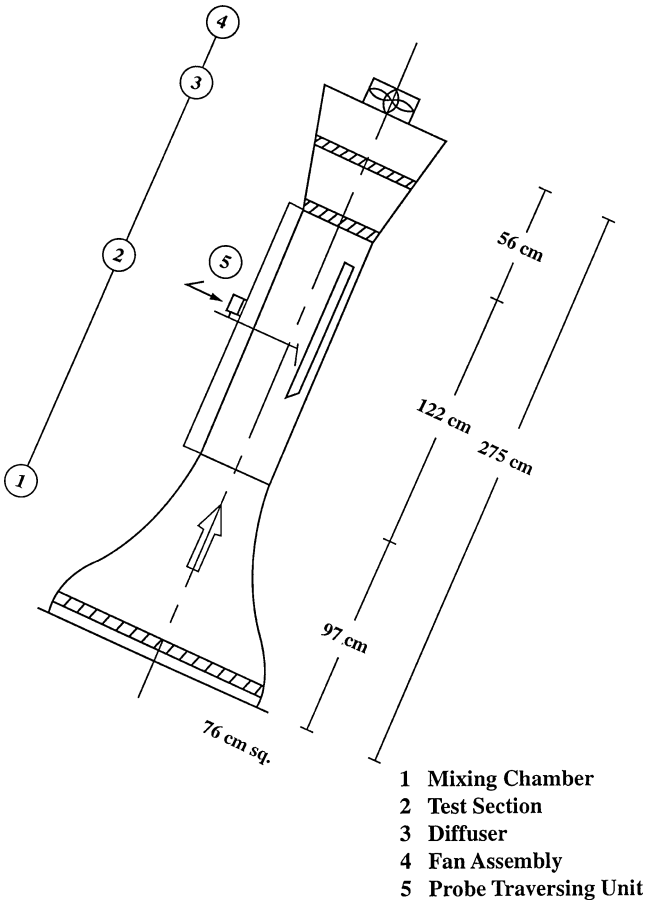

Fig. 1. Schematic diagram of the air tunnel.

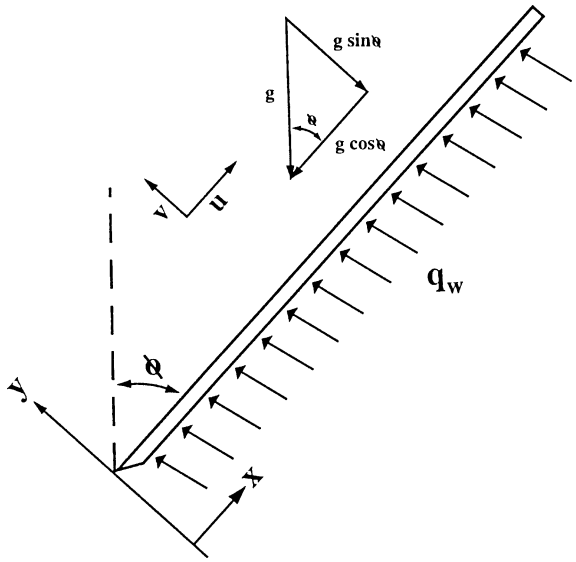

Fig. 2. Schematic diagram of the flat plate geometry.

$0.25 \sim 3.0$ $m{\cdot}s^{-1}$, with a free-stream turbulence intensity of less than 1%. Fig. 2 shows a schematic diagram of the inclined flat plate geometry. The uniform heat flux surface was formed by using a single sheet (0.06 mm thick) of stainless steel foil (29.85 cm wide and 73.66 cm long) glued smoothly to a plexiglass plate (1.27 cm thick) using double-sided tape (0.05 mm thick). To minimize the heat transfer loss by conduction from the back surface of the foil, insulation was added to the back of the plexiglass plate. This insulation consisted of two layers, a balsa wood layer (1.27 cm thick) followed by a Styrofoam layer (5.08 cm thick). The surface temperature of the foil was measured with 30 copper-constantan thermocouples attached to the back surface of the heated foil and distributed along the axial direction. The uncertainties in the measured results were estimated (at the 95% confidence level) according to the procedure outlined by Moffat [9] and they are reported in the appropriate section of this paper. The repeatability of the temperature measurements was 0.2 °C and the error in the stated wall temperature was estimated at ±1 °C.

Electric current was supplied to the foil (test surface) by an 8V–100A D.C. power supply which was connected to copper busbars that were firmly connected to both the

front and back ends of the foil. This arrangement provided a heated surface with a uniform heat flux as was reported by Abu-Mulaweh et al. [8]. The input energy was determined by measuring the current and the voltage drop across the foil. The uncertainty associated with the energy input as determined from these measurements was less than 2%. Energy losses due to thermal radiation from the heated foil and conduction through the back insulation were determined through calibration of the apparatus for both natural convection and also for mixed convection adjacent to vertical flat plate by Abu-Mulaweh [8]. This calibration resulted in determining the thermal resistance of one of the back insulation layers (the balsa wood layer) and the emissivity of the stainless steel foil for the temperature range that is under consideration $20 < T_W < 70\,^{\circ}\mathrm{C}$. The quantities were determined to be equivalent to back resistance $R_b = 0.055\ \mathrm{W{\cdot}m^{-1}{\cdot}\,^{\circ}C^{-1}}$ and emissivity $\varepsilon = 0.055$. The calibration established that the radiation loss from the front side of the plate was less than 10% of the input energy and the heat loss by conduction from the back side of the plate was less than 11% of the total energy input. The convective heat flux for a given steady state condition was then determined by subtracting the conduction and the radiation losses from the input energy to the heated foil. The errors associated with the convective heat flux was established to be less than 3%.

The velocity measurements at any desired location were carried out using a 3-beam, backward scattering, two-component laser-Doppler velocimeter (LDV) and a three-dimensional traversing system. Air temperature measurements were carried out by utilizing a cold wire constant-current anemometer with boundary-layer wire probe. The probe was calibrated frequently to ensure accurate measurements. The repeatability of the mean velocity measurements was determined to be within 2%, and that of the temperature measurements was within 0.25 °C (0.5%).

Flow visualizations were also performed to verify the boundary-layer development and its two-dimensional nature. These flow visualizations were carried out by using a 15-Watt collimated white light beam, 2.5 cm in diameter. Glycerin smoke particles, 2 to 5 microns in diameter, which are generated by immersing a 100 Watt heating element into a glycerin container, are added to the inlet air flow and used as scattering particles for flow visualization and for LDV measurements.

Temperature and velocity distributions were measured simultaneously by adjusting the cold wire probe to be about 2 mm behind the measuring volume of the LDV system. Rapid data acquisition and data reduction for measurements of both temperature and velocity were performed through proper analog to digital converter and software on an IBM AT microcomputer. All fluid properties were evaluated at the film temperature $T_f = (T_W + T_\infty)/2$, where T_W is the local wall temperature.

3. Results and discussion

Flow visualization was performed to establish that a proper laminar boundary layer flow was developing adjacent to the flat plate. Adjustment of air flow suction from the backside of the plate insured that the above condition occurred at each of the flow rates used in this investigation. Measurements of the streamwise velocity component across the width of the tunnel, at various heights above the plate, displayed a wide two-dimensional flow region (about 80% of the width of the heated wall around its center) where the air flow velocity is almost constant (to within 4%) at a fixed distance from the heated wall, thus justifying the two-dimensional flow approximation. Moreover, the boundary layer flow adjacent to the unheated flat plate (pure forced convection, $\xi = 0$) was examined by measuring velocity distributions for different free stream velocities and streamwise locations. Fig. 3 shows the comparison between the measured and the predicted velocity profiles for forced convection. The figure clearly shows that the measurements are in good agreement with the predicted values (Blasius solution), with deviations of less than 2%, thus validating the performance of the air tunnel and its instrumentations. All reported velocity and temperature measurements were taken along the midplane ($z = 0$) of the plate's width, and only after the system had reached steady-state conditions. It should be mentioned that it took 5–6 hours for steady-state to be reached.

Numerical predictions of temperature and velocity distributions utilizing both the local similarity solution model reported by Wilks [10] and the local nonsimilarity solution used by Armaly et al. [11] are compared with measured re-

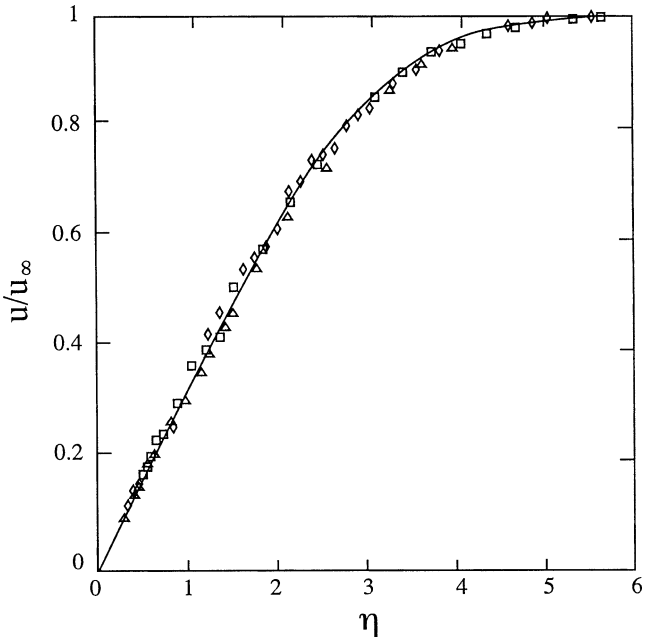

Fig. 3. Comparison between predicted and measured velocity distributions for the unheated plate ($\xi = 0$).

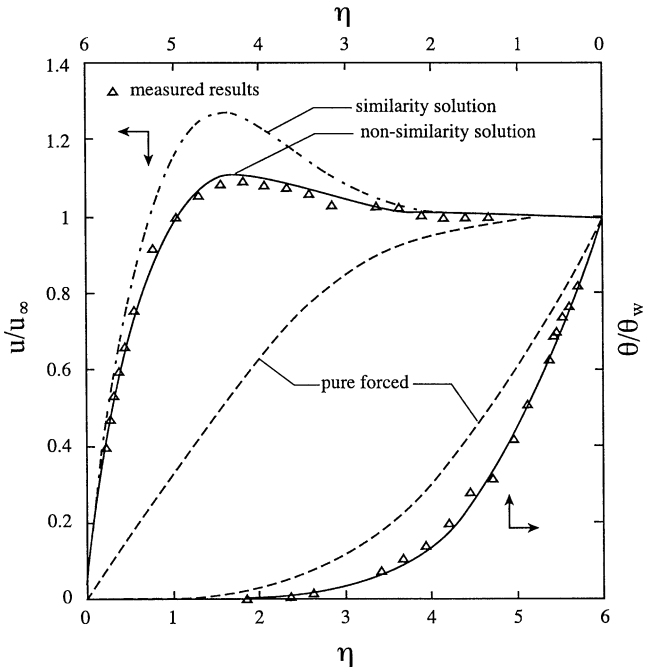

Fig. 4. Measured and predicted velocity and temperature distributions ($\xi = 1.88$).

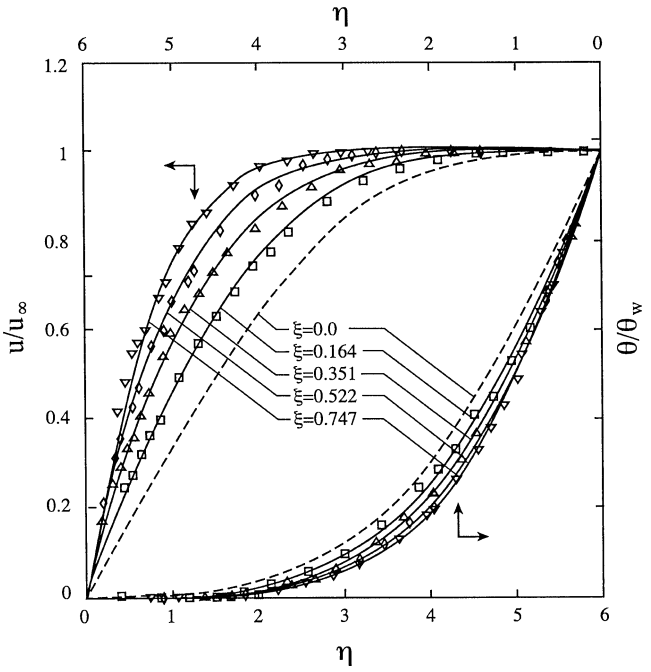

Fig. 5. Measured and predicted velocity and temperature distributions for different buoyancy parameters.

sults in Fig. 4 for the buoyancy parameter $\xi = 1.88$. It is evident from this figure that the velocity distributions predicted by the local nonsimilarity model agree favorably with measured results, but the local similarity model overpredicts both the velocity distributions and the velocity gradients at the wall. The fact that the local similarity method overpredicts the flow field results was also reported by Ramachandran et al. [5,6] and Abu-Mulaweh et al. [8]. On the other hand, predictions of the temperature distributions by both models (i.e., local similarity and local nonsimilarity) are seen to be in good agreement with the experimental values. The uncertainty in η is ± 0.04, in u/u_∞ it is ± 0.02, and in θ/θ_w it is ± 0.025.

The velocity and temperature profiles were measured for buoyancy assisting conditions in the range of buoyancy parameters $0 < \xi < 2.91$. Representative measured temperature and velocity profiles are shown in Figs. 5 and 6. In these two figures the solid lines represent the velocity and temperature profiles predicted by the local nonsimilarity model. The predicted velocity and temperature profiles for pure forced convection, $\xi = 0$, are also included in these figures (dashed lines) for comparison. The figures indicate that the measured velocity and temperature profiles are in very good agreement with the predictions (with less than 4% deviation). These two figures demonstrate clearly the effect of buoyancy force on the flow and thermal fields. As the buoyancy force (i.e., the buoyancy parameter) increases, both the temperature and the velocity gradients at the heated wall increase, causing an increase in both the local Nusselt number and the local friction coefficient. Also, the figures indicate that the flow field is more sensitive to changes in the buoyancy force than the thermal field.

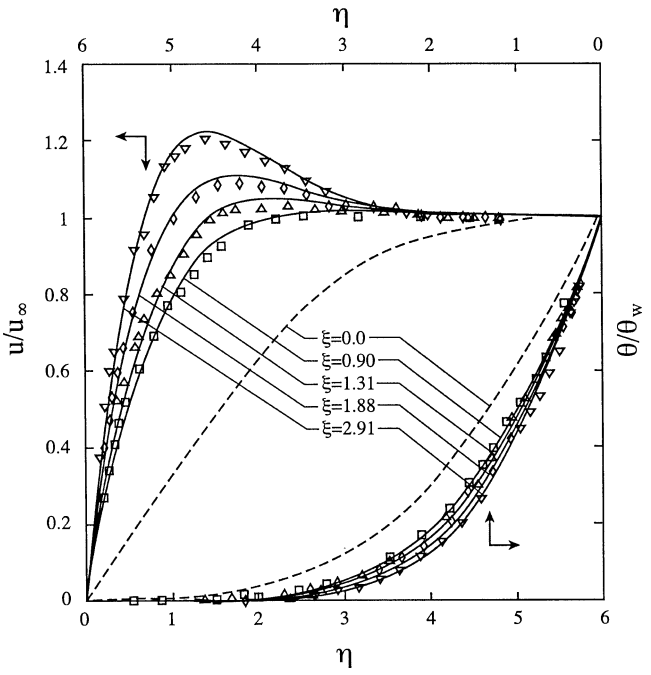

Fig. 6. Measured and predicted velocity and temperature distributions for different buoyancy parameters.

The measured wall temperature distribution and the deduced convective wall heat flux were utilized to calculate the local Nusselt number as defined by:

$$Nu_x = q_w x / \left[k(T_w - T_\infty)\right] \tag{1}$$

Fig. 7 illustrates the variation of the predicted and deduced (measured) local Nusselt number of laminar mixed convection flow adjacent to an inclined surface with uniform heat

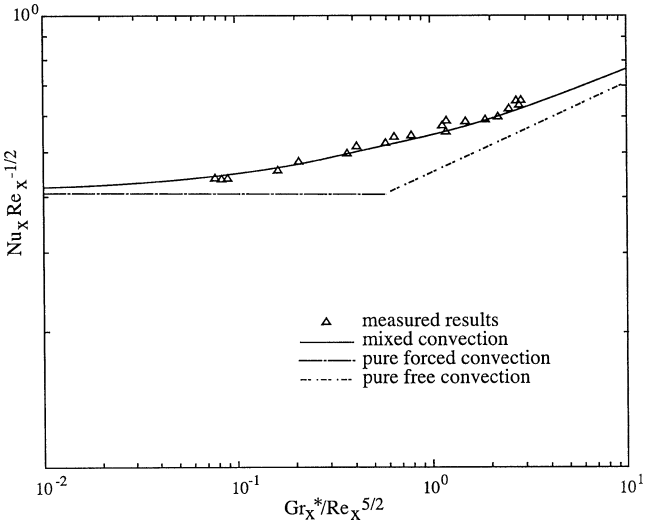

Fig. 7. Measured and predicted local Nusselt number.

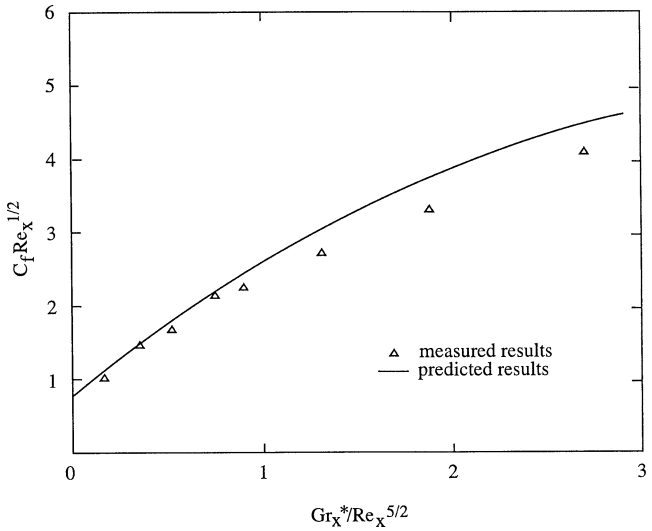

Fig. 8. Measured and predicted local friction coefficient.

flux as a function of the buoyancy parameter. The uncertainty associated with deducing the Nusselt number is 5% and with ξ it is 6%. It can be seen from the figure that the mixed convection local Nusselt number increases as the buoyancy parameter increases (under the buoyancy assisting condition). This increase is due to an increase in the temperature gradient at the heated wall, as shown in Figs. 5 and 6. The local Nusselt numbers in the mixed convection regime from the measurements are in good agreement with the numerical predictions based on the local nonsimilarity model (with less than 6% deviation). Similar results were reported by Abu-Mulaweh et al. [8] for the case of mixed convection flow adjacent to a vertical surface with uniform wall heat flux. Also, the asymptotes for the pure forced convection limit ($\xi = 0$) and the pure free convection limit ($\xi = \infty$) are presented in the figure for comparison. It is clear that the mixed convection local Nusselt numbers are higher than the local Nusselt number for either pure forced or pure free convection flow.

The measured velocity gradient at the heated wall was used to calculate the wall shear stress and the friction coefficient from the following relation:

$$C_f = \mu(\partial u/\partial y)_{y=0}/\left(\rho u_\infty^2/2\right) \tag{2}$$

The variation of the measured and predicted wall shear stress or the local friction coefficient of laminar mixed convection flow adjacent to an inclined surface with uniform heat flux is illustrated in Fig. 8 as a function of the buoyancy parameter. This figure shows that as the buoyancy parameter increases, the local friction coefficient increases. This is because the velocity gradient at the heated wall increases as a result of increasing buoyancy parameter (see Figs. 5 and 6). As can be seen from the figure, good agreement exists between the predicted and the measured values for low buoyancy parameters, but deviations occur as the buoyancy parameter increases. Similar results were reported by Abu-Mulaweh et al. [8] for the case of mixed convection flow adjacent to a vertical surface with uniform wall heat flux. The strong sensitivity of those results to the velocity gradient, and our inability to deduce accurately that quantity when the velocity profile near the wall becomes steeper (i.e., for high buoyancy force), is the cause for the deterioration of the deduced friction coefficients. The uncertainty associated with deducing the friction coefficient is 8%.

4. Conclusion

Measurements of velocity and temperature distributions are reported for laminar mixed convection flow adjacent to an inclined flat plate with uniform surface heat flux for range of buoyancy parameters of $0 < \xi < 2.91$. The mixed convection local Nusselt number and local friction coefficient were deduced from these measurements. It was found that both the mixed convection local Nusselt number and local friction coefficient increase as the buoyancy force increases (under the buoyancy assisting condition). The velocity field was found to be more sensitive to the buoyancy force than the thermal field. Predictions from both local similarity and local nonsimilarity models agree well with the experimental results for the thermal field, but only the predictions from the local nonsimilarity model agree favorably with the measured values for the flow field.

References

[1] H.T. Lin, Y.H. Chen, Analogy between fluid friction and heat transfer of laminar mixed convection on flat plates, Internat. J. Heat Mass Transfer 37 (1994) 1683–1686.

[2] W.R. Risbeck, T.S. Chen, B.F. Armaly, Laminar mixed convection over horizontal flat plate with power-law variation in surface temperature, Internat. J. Heat Mass Transfer 36 (1993) 1859–1866.

[3] N.G. Kafoussias, D.A.S. Rees, J.E. Daskalakis, Numerical study of the combined free-forced convective laminar boundary layer flow past a vertical isothermal flat plate with temperature-dependent viscosity, Acta Mech. 127 (1998) 39–50.
[4] I.A. Hassanein, F.S. Ibrahim, R.S.R. Gorla, Mixed convection boundary layer flow of a micropolar fluid on a horizontal plate, Chem. Engrg. Commun. 170 (1998) 117–131.
[5] N. Ramachandran, B.F. Armaly, T.S. Chen, Measurements and predictions of laminar mixed convection flows adjacent to a vertical surface, J. Heat Transfer 107 (1985) 636–641.
[6] N. Ramachandran, B.F. Armaly, T.S. Chen, Measurements of laminar mixed convection flow adjacent to an inclined surface, J. Heat Transfer 109 (1987) 146–150.
[7] S.S. Moharreri, B.F. Armaly, T.S. Chen, Measurements in the transition vortex flow regime of mixed convection above a horizontal heated plate, J. Heat Transfer 110 (1988) 358–365.
[8] H.I. Abu-Mulaweh, B.F. Armaly, T.S. Chen, Measurements of laminar mixed convection adjacent to a vertical plate—uniform wall heat flux case, J. Heat Transfer 114 (1992) 1057–1059.
[9] R.J. Moffat, Describing the uncertainties in experimental results, Exp. Therm. Fluids Sci. 1 (1988) 3–17.
[10] G. Wilks, Combined forced and free convection flow on vertical surfaces, Internat. J. Heat Mass Transfer 16 (1973) 1958–1964.
[11] B.F. Armaly, T.S. Chen, N. Ramachandran, Correlation for laminar mixed convection on vertical, inclined and horizontal flat plate with uniform heat flux, Internat. J. Heat Mass Transfer 30 (1987) 405–408.